Journal of Climate

Interhemispheric influence of the northern summer monsoons on the southern subtropical anticyclones

--Manuscript Draft--

Manuscript Number:	JCLI-D-13-00106
Full Title:	Interhemispheric influence of the northern summer monsoons on the southern subtropical anticyclones
Article Type:	Article
Corresponding Author:	Sang-Ki Lee, Ph.D. University of Miami Miami, FL UNITED STATES
Corresponding Author's Institution:	University of Miami
First Author:	Sang-Ki Lee, Ph.D.
Order of Authors:	Sang-Ki Lee, Ph.D.
	Carlos R. Mechoso, Ph.D.
	Chunzai Wang, Ph.D.
	J. David Neelin, Ph.D.
Abstract:	The southern subtropical anticyclones are notably stronger in the austral winter than in summer, particularly over the Atlantic and Indian Ocean basins. This is in contrast with the Northern Hemisphere (NH), in which subtropical anticyclones are more intense in summer according to the "monsoon heating" paradigm. To better understand the winter intensification of southern subtropical anticyclones, the present study explores the interhemispheric response to monsoon heating in the NH during the austral winter. A specially designed suite of numerical model experiments is performed in which summer monsoons in the NH are artificially weakened. These experiments are performed with both an atmospheric general circulation model and a simple two-layer model. The highlight of our findings is that during the boreal summer enhanced tropical convection activity in the NH plays important roles in either maintaining or strengthening the southern subtropical anticyclones. Enhanced NH convection largely associated with the major summer monsoons produces subsidence over the equatorial oceans and the tropical Southern Hemisphere via interhemispheric meridional overturning circulations and increases the sea level pressure locally. In addition, suppressed convection over some regions of climatological subsidence produces stationary barotropic Rossby waves that propagate far beyond the tropics. These stationary barotropic Rossby waves and those forced directly by the summer heating in the NH are spatially phased to strengthen the southern subtropical anticyclones over all three oceans. The interhemispheric response to the NH summer monsoons is most dramatic in the South Pacific, where the subtropical anticyclone nearly disappears in the austral winter without the influence from the NH.

Powered by Editorial Manager® and ProduXion Manager® from Aries Systems Corporation

Page and Color Charge Estimate Form

Click here to download Page and Color Charge Estimate Form: Page_Charge_Estimation_Form.pdf

Click here to download Response to Reviewers: reply_reviewer.pdf

Reviewer #2: I thank the authors for exploring the role of the basic state meridional velocity on wave propagation, however, it appears that the simple model experiments are considering only part of the total wave change from SYNC to CTRL. Currently the authors only consider the response to anomalous heating (i.e. heating in CTRL minus SYNC) under the SYNC background state. But the changes in the background state almost certainly have an effect too. Therefore, the authors also need to consider the response to anomalous heating under the CTRL background state.

In their reply the authors argued that prescribing a CTRL background state is not appropriate: "...the simple model is forced by the heat sources and sinks (equivalently mass sources and sinks) that drive the interhemispheric Hadley circulation shown in Figure 5c. Therefore, the simple model should reproduce this interhemispheric Hadley circulation in the model solution. This means that prescribing the Hadley circulation in JJA taken from the NCEP-NCAR reanalysis as the background state in the simple model is not appropriate because a great portion of the Hadley circulation in JJA is actually simulated by the simple model."

This is not true because the simple model is linear. Therefore, the changes in the Hadley cell in the simple model have absolutely no effect on the waves in the simple model. The only way to understand the role of the background state on the Rossby waves in the simple model is to prescribe the new background state. Also, a portion of the response comes from the new CTRL background state acting on the climatological heating.

Reply: We greatly appreciate this suggestion. In the previous version of our manuscript, the interhemispheric heating and cooling (Fig. 8) is prescribed in the two-level atmosphere model with the background states derived from SYNC. This model result provides the first order response of the equatorially symmetric atmosphere (i.e., SYNC) to the interhemispheric forcing. In this sense, we believe that the design of our simple model experiments is proper given that the model used is a linear model.

However, we agree with the reviewer that the cross-hemispheric Hadley cell in summer can enhance the propagation of stationary waves to the SH across the equator. The suggestion from the reviewer is to perform additional simple model experiments by using the background states derived from CTRL instead of those derived from SYNC. We agree with the reviewer that such experiments could help us to better understand the effect of the cross-hemispheric Hadley cell on the propagation of stationary waves to the SH. We have performed these additional experiments suggested by the reviewers, and Fig.1 0, 11 and 12 are replaced using the new experiments (i.e., background states are derived from CTRL) as requested.

As shown in new Fig. 10 and old Fig. 10, the result from the new experiment (i.e., background states are derived from CTRL) is overall consistent with that from the original model experiment (i.e., background states is derived from SYNC). As shown in new Fig. 11 and old Fig. 11, the model responses to the anomalous cooling in the South-central Pacific Ocean, the western equatorial Atlantic, and the equatorial Indian Ocean are also consistent between the original and the new sets of experiments. Similarly, new Fig. 12 and old Fig. 12 show that the model responses to the anomalous heating over the northwestern Pacific Ocean and the WHWP are also consistent between the original and the new sets of experiments.

When the simple model is forced by anomalous heating associated with the Indian Summer Monsoon (ISM), the spatial pattern of the response is somewhat similar between the original and the new experiment. However, the amplitude of the response is much greater especially over the South Pacific Ocean in the new experiment. This suggests that the cross-hemispheric Hadley cell in CTRL enhances the propagation of the ISM-forced stationary waves to the SH across the equator. To confirm it, this experiment is repeated without the baroclinic background meridional winds. As shown in Fig. R1 (attached below), without the baroclinic background meridional winds across the equator (i.e., the interhemispheric overturning circulation), the stationary waves forced in the ISM region hardly propagate to the SH, in line with the explanation offered by Watterson and Schneider (1987). The manuscript is revised according to these findings from the new experiments.

Minor comment:

Line 14 on page 10: The authors need to modify the following statement to take into account the role of background meridional wind: "The band of easterlies in the tropics does not allow stationary Rossby waves to propagate across the equator (e.g., Branstator 1983)."

Reply: This sentence is now changed to "The band of easterlies in the tropics makes it difficult for stationary Rossby waves to propagate across the equator (e.g., Branstator 1983)."

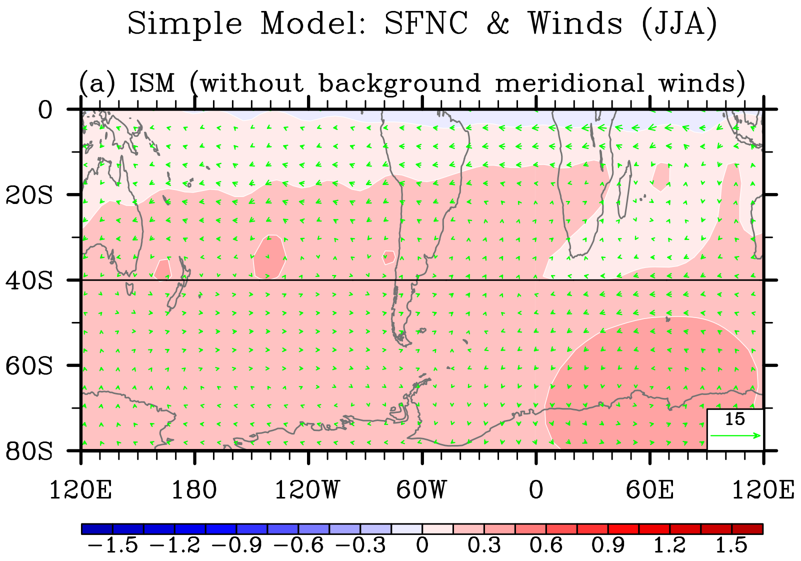

Figure R1. Barotropic stream function and wind vector responses in the simple model experiment to diabatic heating in the Indian summer monsoon region. The baroclinic background meridional winds are not used in this experiment. Compare this plot with Figure 12c. The units are 10^{7} m^{2} s^{-1} for stream function, and m s^{-1} for wind vector.

Manuscript with track changes
Click here to download Additional Material for Reviewer Reference: lee_etal_2013_jcl_text_2nd_revision_with_track_changes.doc

Manuscript (text)
Click here to download Manuscript (non-LaTeX): lee_etal_2013_jcl_text_2nd_revision.doc

Interhemispheric Influence of the Northern Summer Monsoons on the Southern Subtropical Anticyclones

Sang-Ki Lee[1,2], Carlos R. Mechoso[3], Chunzai Wang[2], and J. David Neelin[3]

[1]Cooperative Institute for Marine and Atmospheric Studies, University of Miami, Miami FL

[2]Atlantic Oceanographic and Meteorological Laboratory, NOAA, Miami FL

[3]Department of Atmospheric and Oceanic Sciences, University of California, Los Angeles, Los Angeles, CA

Revised and resubmitted to Journal of Climate (2nd revision)

August 2013

Corresponding author address: Dr. Sang-Ki Lee, NOAA/AOML, 4301 Rickenbacker Causeway, Miami, FL 33149, USA. E-mail: Sang-Ki.Lee@noaa.gov.

Abstract

The southern subtropical anticyclones are notably stronger in the austral winter than in summer, particularly over the Atlantic and Indian Ocean basins. This is in contrast with the Northern Hemisphere (NH), in which subtropical anticyclones are more intense in summer according to the “monsoon heating” paradigm. To better understand the winter intensification of southern subtropical anticyclones, the present study explores the interhemispheric response to monsoon heating in the NH during the austral winter. A specially designed suite of numerical model experiments is performed in which summer monsoons in the NH are artificially weakened. These experiments are performed with both an atmospheric general circulation model and a simple two-layer model. The highlight of our findings is that during the boreal summer enhanced tropical convection activity in the NH plays important roles in either maintaining or strengthening the southern subtropical anticyclones. Enhanced NH convection largely associated with the major summer monsoons produces subsidence over the equatorial oceans and the tropical Southern Hemisphere via interhemispheric meridional overturning circulations and increases the sea level pressure locally. In addition, suppressed convection over some regions of climatological subsidence produces stationary barotropic Rossby waves that propagate far beyond the tropics. These stationary barotropic Rossby waves and those forced directly by the summer heating in the NH are spatially phased to strengthen the southern subtropical anticyclones over all three oceans. The interhemispheric response to the NH summer monsoons is most dramatic in the South Pacific, where the subtropical anticyclone nearly disappears in the austral winter without the influence from the NH.

1. Introduction

In our current understanding, the principal driver of the subtropical anticyclones (also known as the subtropical highs) varies with season. This principal driver is heating associated with the monsoons over the adjacent continents during the summer season, and orographic effects on the trade easterlies and mid-latitude westerlies during the winter season. Rodwell and Hoskins (2001; hereafter RH01) argued that the monsoon heating generates a Kelvin wave response over the ocean to the east forming the equatorward portion of the subtropical anticyclone with a poleward low-level jet to satisfy Sverdrup balance. The heating also generates a Rossby wave response that produces adiabatic descent over regions to the west (Rodwell and Hoskins 1996). An equatorward low-level jet forms to satisfy Sverdrup balance closing off the subtropical anticyclone on its eastern flank. Additional effects, such as intense near-surface sensible heating over continents and air-sea interactions involving cold sea surface temperatures (SSTs) and low-level clouds in the eastern part of the oceans, also contribute to drive the subtropical anticyclones in the summer season (e.g., Seager et al. 2003; Liu et al. 2004; Miyasaka and Nakamura 2005). In the winter season, monsoon heating is absent and the subtropical anticyclones weaken. Consistent with this line of reasoning, the subtropical anticyclones in the Northern Hemisphere (NH) are stronger and better defined in the boreal summer than in winter (see Fig. 1 obtained with data from the NCEP-NCAR reanalysis). See Ting (1994), Chen et al. (2001) and Chen (2003) for further discussions on the stationary wave response to summer monsoon heating in the NH.

The subtropical anticyclones in the Southern Hemisphere (SH) behave in a qualitatively different manner: They are notably stronger in the austral winter than in summer over the Atlantic and Indian Oceans (see Fig. 1). This could be due to a combination of monsoons being less important generators of zonal asymmetries in the mostly ocean-covered SH, and of topographic effects becoming stronger in winter as the flow intensifies. The former is plausible because the summertime subtropical anticyclones are significantly stronger in the NH than in the SH (Miyasaka and Nakamura 2010). However, an argument based on the seasonality of the SH is questionable because the SH has weaker seasonal variability. Furthermore, although the Andes cordillera is high and has strong slopes, the topography over southern Africa and Australia is relatively low and has a weaker blocking effect on the mean westerly flow (Richter and Mechoso 2004; 2006).

Some revision of the RH01 conceptual model is, therefore, needed to address the seasonality of the southern subtropical anticyclones. Recent studies with numerical models have provided some guidance for such a revision. Wang et al. (2010) used an atmospheric general circulation model (AGCM) to demonstrate that convection over the Western Hemisphere warm pool (WHWP) during the boreal summer (austral winter) can produce adiabatic subsidence over the southeastern tropical Pacific, and thus contribute to maintaining the equatorward portion of the South Pacific subtropical anticyclone and the equatorward low-level jet along the South American coast. In addition, Wang et al. (2010) showed, by performing experiments with the simple two-level atmospheric model developed by Lee et al. (2009), that the interhemispheric connection between the WHWP and the South Pacific subtropical anticyclone depends critically on the configuration of the mean zonal winds in the SH. Richter et al. (2008) demonstrated a similar interhemispheric connection between the African - Indian summer monsoon and the South Atlantic subtropical anticyclone by comparing simulations by two versions of the University of California, Los Angeles (UCLA) AGCM that reproduce climate features with significantly different success.

On the basis of the studies by Wang et al. (2010) and Richter et al. (2008) one could advance the following conjecture. *Interhemispheric teleconnections associated with the major summer monsoons and deep tropical convection over warm SSTs in the NH contribute to the wintertime strengthening of the southern subtropical anticyclones*. The present study examines this conjecture. Our goals are to explore to what extent the southern subtropical anticyclones during the austral winter are affected by the major monsoons and deep tropical convection in the NH and to gain insight on the underlying mechanisms at work for the teleconnections. To achieve these goals we perform and analyze a suite of specially designed AGCM simulations complemented by additional experiments using a simple atmosphere model.

In evaluating the SH subtropical anticyclone response to NH convection, we focus primarily on sea level pressure (SLP). SLP will have contributions arising from both baroclinic and barotropic dynamics, and can be made precise in models that carry out a vertical mode decomposition (e.g., Lee et al. 2009; Neelin and Zeng 2000). In these, the first baroclinic mode has high surface pressure and cool tropospheric temperature in regions of upper-level convergence and adiabatic subsidence, and low surface pressure and warm tropospheric temperature in regions of diabatic heating. The baroclinic Rossby wave response to monsoon heating is at the core of the RH01 conceptual model, but can in turn excite barotropic Rossby waves via several interaction mechanisms: vertical wind shear and surface stress acting on the baroclinic mode, and vertical advection of baroclinic mode vorticity (e.g., Lee et al. 2009; Ji et al. 2013). The barotropic mode contribution to subtropical SLP can thus have significantly different teleconnection characteristics than the direct baroclinic mode contribution.

In section 2 we present our research strategy, give a brief description of the AGCM we use, and list the AGCM simulations we performed. Next, using the AGCM results, we describe the

SLP response in the SH over each ocean basin to the major summer monsoons in the NH. In sections 4 and 5, we analyze the AGCM simulations. We then posit that the major summer monsoons in the NH force interhemispheric meridional overturning circulation, and the diabatic cooling over certain sinking regions forces stationary barotropic Rossby waves in the extratropical SH to enhance the southern subtropical anticyclones. In section 6, this hypothesis is supported by specially designed experiments with the simple two-level model of Lee et al. (2009). Section 7 provides a summary and discussion.

2. Strategy, model, and experiments

Our strategy in this study is based on performing AGCM runs in which a control simulation (CTRL) is compared to an idealized experiment with artificially weakened summer monsoons in the NH (SYNC). This weakening in SYNC is achieved by shifting both the insolation at the top of the atmosphere (TOA) and the SSTs and sea ice cover in the NH by one-half the seasonal cycle (6 months) i.e., by synchronizing the seasonal cycles in the model's external and boundary conditions across hemispheres (See Fig. 2). In SYNC, therefore, there is a global warm season in December-February (DJF) and a global cold season in June-July (JJA), which, in the calendar year, correspond to those in the SH.

We use the NCAR Community Atmospheric Model version 4 (CAM4). CAM4 is a global atmosphere-land model with prescribed SSTs and sea ice cover (Neale et al. 2012). The finite volume dynamic core has a horizontal resolution of 2.5° (zonal) $\times$ 1.9° (meridional) and 26 hybrid sigma-pressure layers. AGCM runs are 20-years long, of which the first five years are discarded to minimize any possible transient spinup effects. The time mean of the remaining 15 years is analyzed in the following sections.

3. Results

Figure 3 shows the mean SLP obtained in CTRL for DJF and JJA. The simulated subtropical anticyclones are realistic, but are generally stronger than in the NCEP-NCAR reanalysis (see Fig. 1). The simulation captures two important features of the subtropical anticyclones: 1) those in the NH are better defined in the boreal summer than in winter, and 2) those in the SH remain quite strong and well defined in the austral winter. In view of these results, it is reasonable to conclude that CAM4 is an appropriate tool for the present study.

Figure 4 shows time-latitude plots of monthly-mean, zonally averaged SLP over the South Pacific, South Atlantic and South Indian Oceans from the NCEP-NCAR reanalysis, CTRL and SYNC. The zonal average is carried out from the eastern to the western boundaries of the respective ocean basin.

Starting with the South Pacific, the maximum SLPs in both the NCEP-NCAR reanalysis and CTRL occurs during the austral spring (August-November; Figs. 4a and d). In SYNC, however, when the interhemispheric effect is removed, (Fig. 4g), the maximum SLPs occur in DJF and the minimum in July - August. This latter feature of the seasonal cycle is consistent with the monsoon heating mechanism of RH01. This suggests that the NH heating is a key contributor to the strength of the subtropical anticyclone over the South Pacific during the austral winter.

For the South Atlantic and South Indian Oceans, the maximum SLPs in both the NCEP-NCAR reanalysis and CTRL occurs around July - August (Figs. 4b and e). In SYNC (Fig. 4h), the maximum SLP occurs a little earlier with a much weaker magnitude than in CTRL (Fig. 4e). This suggests again that the NH heating plays a major role in the strengthened subtropical anticyclones over the South Atlantic and South Indian Oceans during the austral winter. It is interesting to note that the maximum SLPs still does not occur in the austral summer, suggesting that the subtropical anticyclones over the South Atlantic and South Indian Oceans could be still strengthened during the austral winter without the NH heating. A potential mechanism that may explain this seasonal cycle in SYNC is discussed in section 7.

In summary, the AGCM experiments indicate that the interhemispheric response to the NH heating plays a crucial role in either maintaining or strengthening the southern subtropical anticyclones in the austral winter. The interhemispheric response is very strong over all three oceans, but it is more dramatic in the South Pacific, where the subtropical anticyclone nearly disappears in the austral winter without the influence from the NH. In the following sections we explore the physical processes that determine the interhemispheric response to the heating in the NH and its impact on the southern subtropical anticyclones.

4. Interhemispheric meridional overturning circulation

In CTRL, the mean Hadley circulation during JJA (Fig. 5a) shows rising motion in the tropical NH and sinking motion in the tropical SH. In SYNC, with external and boundary forcings in the NH corresponding to DJF, this configuration changes drastically (Fig. 5b). Instead, there is a pair of "Hadley cells" with rising motion near the thermal equator at around 5°N and sinking motion in the latitude band between 15° and 30° of each hemisphere. The difference in the Hadley circulations between CTRL and SYNC (Fig. 5c) is the net meridional overturning circulation forced by the NH heating during the warm season of that hemisphere. The net interhemispheric meridional overturning circulation shown in Fig. 5c is, in general, consistent with the suggestion on the association between the seasonal cycle of the Hadley cell and the monsoons put forward by Dima and Wallace (2003).

Associated with the net interhemispheric meridional overturning circulation (Fig. 5c) is the upper-level convergence field over the tropical SH. At the convergence centers subsiding air tends to yield local SLP increases (e.g., Rodwell and Hoskins 1996). It is important to point out, however, that the extent of the sinking branch of the net interhemispheric meridional overturning circulation is limited to the deep tropics equatorward of around 20°S (Fig. 5c). Therefore, the strengthening of the southern subtropical anticyclones south of around 20^{o}S cannot be simply explained as the direct result of the net interhemispheric meridional overturning circulation forced from the NH.

Figure 6 shows the mean velocity potential and divergent winds during JJA at 200 hPa for CTRL, SYNC and CTRL - SYNC. In CTRL, divergent winds (rising motions) occur over India and East Asia, in association with the local summer monsoon, the northwestern tropical Pacific, and the WHWP, whereas convergent winds (sinking motions) occur over the southeastern tropical Pacific and much of the Atlantic especially the tropical South Atlantic (Fig. 6a). When the interhemispheric effect is removed (i.e. SYNC), the centers of rising motion in the NH are shifted toward the equator over the western equatorial Atlantic Ocean and the equatorial Indian Ocean (Fig. 6b). Therefore, the net result of the interhemispheric response to the heating in the NH is to produce subsidence over the western equatorial Atlantic Ocean and the equatorial Indian Ocean (Fig. 6c).

In addition, a broad region of subsidence exists in CTRL – SYNC over the south-central tropical Pacific, the southeastern tropical Pacific, and the tropical South Atlantic. It appears that the subsidence in the south-central tropical Pacific is linked mainly to the summer expansion of the western Pacific warm pool in the region of the northwestern tropical Pacific. The subsidence in the southeastern tropical Pacific appears to be linked to the WHWP consistent with Wang et al. (2010), whereas the subsidence over the tropical South Atlantic appears to be linked to the Indian and West African summer monsoons, as suggested by Richter et al. (2008), and also to the WHWP. These effects occur essentially as baroclinic mode teleconnections, which have no trouble crossing the equator, but tend to remain trapped within the equatorial wave guide (Gill 1980). In the next two sections, we turn to potential barotropic contributions.

5. Propagation of stationary Rossby waves to the subtropics

As shown in Fig. 7a, the interhemispheric effect on SLP is not limited to the tropical SH where the sinking branch of the net interhemispheric meridional overturning circulation directly increases the local SLPs. Over the regions of subsidence in the equatorial oceans and the tropical SH, slowly sinking air is heated by adiabatic compression and thus limits the vertical development of convection. Therefore, the sinking regions in the south-central Pacific Ocean, the western equatorial Atlantic Ocean, and the equatorial Indian Ocean are characterized by suppressed moist convective heating rate at 500 hPa (Figure 8) and reduced convective precipitation rate (not shown). Potentially, the diabatic cooling (i.e., reduced diabatic heating relative to SYNC) over these regions can produce stationary barotropic Rossby waves far beyond the tropics (e.g., Hoskins and Karoly 1981; Horel and Wallace 1981; Branstator 1983; Sardeshmukh and Hoskins 1988; Ting and Held 1990; Lee et al. 2009). Consistent with this hypothesis, the spatial pattern of SLPs in response to the interhemispheric teleconnections closely resembles the stream function response at 500 hPa, which is a widely used proxy to identify stationary barotropic Rossby waves (Fig. 7b). Note that the stream function sign is reversed (i.e., circulation is anticlockwise around positive stream function) for a better visual comparison with the SLP (Fig. 7a). It is important to point out that, due to cold SSTs and low level clouds, conditions are not suitable for deep convection in the southeastern tropical Pacific or the southeastern tropical Atlantic. Therefore, the subsidence in these regions directly increases the SLPs locally, but cannot induce diabatic cooling (Fig. 8) or force stationary barotropic Rossby waves to the extratropical SH.

6. Simple model experiments

We next qualitatively examine the interpretation we have given to the differences between CTRL and SYNC, particularly to the forcing of stationary barotropic Rossby waves shown in Fig. 7b by diabatic cooling (i.e., reduced diabatic heating relative to SYNC) in the equatorial oceans and the tropical SH. For such examination we select the simple atmospheric model of Lee et al. (2009). This is a two-level, minimal complexity model of both the local and remote stationary responses of the atmosphere to tropical heating anomalies. The model equations are linearized about background wind fields, and recast as baroclinic and barotropic components with thermal advection in the tropics neglected. See Lee et al. (2009) and Wang et al. (2010) for more details about this model.

The band of easterlies in the tropics makes it difficult for stationary Rossby waves to propagate across the equator (e.g., Branstator 1983). This is particularly true if the stationary barotropic Rossby waves are forced in the tropical NH during the boreal summer when the zonal background barotropic flow is mainly westward equatorward of around 20°N (Pexoto and Oort 1992). In the simple model experiments of Wang et al (2010), however, diabatic heating in the tropical NH directly influences the SH without invoking the associated diabatic cooling. In Wang et al. (2010), the baroclinic response to diabatic heating in the tropical NH comprises two centers of low SLP anomalies, one in the northwest and the other in the southwest of the forcing region, consistent with the simple Gill model (Matsuno 1966; Gill 1980). As further investigated by Ji et al. (2013), the low SLP anomaly southwest of the forcing region in the tropical NH can be positioned in the tropical SH with a weaker amplitude compared to its counterpart in the NH. Also according to Ji et al. (2013), the Gill-type baroclinic circulations in the tropical SH may in turn interact with the background flows in this hemisphere to produce stationary barotropic Rossby waves.

Additionally, Watterson and Schneider (1987) suggested that a meridional background wind associated with the Hadley circulation could enable wave propagation across the equator even under an easterly background wind. Dima et al. (2005) analyzed the NCEP-NCAR reanalysis to find some supporting evidences. Kraucunas and Hartmann (2007), and Liu and Wang (2013) further demonstrated this mechanism using a nonlinear shallow-water model, and a linearized simple two-level model, respectively.

An important implication drawn from the above-mentioned studies is that summertime diabatic heating in the tropical NH can directly force stationary barotropic Rossby waves in the extratropical SH, without invoking the associated diabatic cooling in the equatorial oceans and the tropical SH, and thus can directly affect the southern subtropical anticyclones. Therefore, it is important to address how effectively the diabatic heating in the tropical NH can directly induce stationary barotropic Rossby waves in the extratropical SH.

In order to address these issues and also to further explore how the heating in the tropical NH and the cooling in the equatorial oceans and the tropical SH considered separately in six major forcing regions (see Fig. 8) affect the southern subtropical anticyclones, we performed seven experiments using the two-level model. In the first experiment, the moist convective heating rate at 500 hPa for JJA obtained from CTRL – SYNC (Fig. 8) is prescribed. The other six experiments are identical to the first, except that the thermal forcing is prescribed only over selected regions (see Fig. 8). In the second, third and fourth experiments, the moist convective heating rate is prescribed only in the south-central Pacific (150°E - 130°W and 20°S - 5°N), the western equatorial Atlantic (60°W - 10°W and 10°S – 7.5°N), and the equatorial Indian Ocean (60°E - 110°W and 20°S - 10°N), respectively. In the fourth, fifth and sixth experiments, the moist convective heating rate is prescribed only in the northwestern Pacific Ocean affected by summer expansion of the western Pacific warm pool (110°E – 160°W and 5°N - 30°N), the WHWP (100°W - 60°W and 5°N - 20°N), and the Indian summer monsoon region (20°W - 110°E and 10°N - 30°N), respectively. See Fig. 8 for the regions of forcing and the heating rates prescribed for these experiments.

For all seven experiments, the background fields are the zonally averaged climatological stream function and velocity potential for JJA in the upper and lower troposphere derived from CTRL. The simple two-level model assumes that barotropic divergence is zero (Lee et al. 2009). Thus, the model is prescribed with only the baroclinic background velocity potential, which is directly related to the Hadley cell in CTRL (Fig. 5a), and with both the barotropic and baroclinic background stream functions. The zonally averaged barotropic and baroclinic background zonal winds and the zonally averaged baroclinic meridional winds (computed from the stream function and velocity potential fields) derived from SYNC and CTRL are shown in Fig. 9 along with those derived from the NCEP-NCAR reanalysis. Since the simple model mainly solves a set of linearized equations, nonlinear effects are not considered in our experiments.

Figure 10 shows the barotropic stream function response to the thermal forcing shown in Fig. 8. The stream function sign is again reversed (i.e., circulation is anticlockwise around positive stream function) for a better visual comparison with the SLP in the AGCM experiments (Fig.

7a). The simple two-level model is an oversimplification of the real atmosphere, and is unable to reproduce the exact shape or propagation pathway of the stationary Rossby waves simulated by CAM4 (Fig. 7b). Nevertheless, a comparison between Figs. 7b and 10 reveals several important common features. In particular, the anticyclones are roughly in place to enhance the southern subtropical anticyclones in all three oceans.

Figure 11a, b and c show the barotropic stream function response to diabatic cooling in the south-central Pacific Ocean, the western equatorial Atlantic Ocean, and the equatorial Indian Ocean, respectively. It is clear that the stationary barotropic Rossby waves originating from the south-central Pacific greatly strengthen the South Pacific subtropical anticyclone. Similarly, the stationary barotropic Rossby waves originating from the western equatorial Atlantic Ocean propagate to the extratropical South Atlantic and strengthen the South Atlantic subtropical anticyclone. It appears that diabatic cooling in the equatorial Indian Ocean and the associated stationary waves contribute to the strength of the South Indian subtropical anticyclone particularly to the south and west of Australia.

Figure 12a, b and c show the barotropic stream function response to diabatic heating in the northwestern Pacific Ocean, the WHWP, and the Indian summer monsoon region, respectively. Unlike those forced in the south-central Pacific Ocean, the stationary barotropic Rossby waves forced in the northwestern Pacific Ocean hardly influence the southern subtropical anticyclones. The stationary waves directly forced in the WHWP only weakly influence the South Pacific subtropical anticyclone.

However, it is interesting to note that the stationary waves directly forced in the Indian summer monsoon region have large influences on the South Pacific and South Atlantic subtropical anticyclones. This experiment is repeated without the baroclinic background meridional winds to find that the baroclinic background meridional winds across the equator (i.e., interhemispheric overturning circulation) play an important role in enhancing the propagation of the Indian summer monsoon-forced stationary waves to the SH, in line with the explanation offered by Watterson and Schneider (1987).

In summary, the simple model experiments support our hypothesis that, in response to the heating in the tropical NH, diabatic cooling occurs in the equatorial oceans and the tropical SH, and the cooling in the equatorial oceans and the tropical SH in turn force the stationary barotropic Rossby waves shown in Fig. 7b, and thus strengthens the southern subtropical anticyclones. The simple model experiments suggest that diabatic heating in the Indian summer monsoon region can also enhance the South Pacific and South Atlantic subtropical anticyclones without invoking the cooling in the equatorial oceans and the tropical SH.

In interpreting these barotropic Rossby wave trains, it should be recalled that they are excited in the simple model by the prescribed diabatic heating or cooling (see Lee et al. 2009). The diabatic cooling is itself a teleconnected response to heating in the tropical NH and is primarily a reduction in deep convective heating that could potentially occur in certain locations over the equatorial oceans and the tropical SH if the tropical NH heating were absent. It is also important to recall that the simple two-level model does not include moist processes. Therefore, unless prescribed, the simple model cannot simulate diabatic processes such as radiative cooling or convective heating. See an intermediate complexity model study by Ji et al. (2013) for further discussions on interhemispheric teleconnections in response to a localized heat source in the tropical NH via the baroclinic mode affecting moist processes and thus convective heating in the tropical SH.

7. Summary and discussions

The present study examines the conjecture that major summer monsoons in the NH contribute to the wintertime strengthening of the southern subtropical anticyclones through interhemispheric teleconnections. To explore this conjecture, we perform a specially designed suite of AGCM experiments in which summer monsoons in the NH are artificially weakened. To elucidate the underlying mechanisms at work for the teleconnections we also perform several experiments using the simple numerical two-level model of Lee et al. (2009).

The results obtained in the AGCM and simple model experiments suggest that the interhemispheric response to the heating in the NH does play a crucial role in either maintaining or strengthening the southern subtropical anticyclones in the austral winter. Although the interhemispheric response is very strong over all three oceans, it is more dramatic in the South Pacific since subtropical anticyclone over this ocean nearly disappears in the austral winter without the influence from the NH.

The sketch in Figure 13 encapsulates results from several parts in the text. During the boreal summer, the interhemispheric meridional overturning circulation is fueled from three hot spots in the tropical NH. These spots are located over the Indian - East Asian summer monsoon region, the northwestern tropical Pacific region affected by summer expansion of the western Pacific warm pool, and the WHWP (see Fig. 6). The associated subsidence and SLP increases occur over the western equatorial Atlantic Ocean, the equatorial Indian Ocean, the south-central tropical Pacific Ocean, the southeastern tropical Pacific Ocean, and the South Atlantic Ocean. Since conditions are suitable for deep convection in the western equatorial Atlantic Ocean, the equatorial Indian Ocean, and the south-central tropical Pacific Ocean due to warm SSTs therein, the subsidence over these three regions suppresses convection (see Fig. 8). The diabatic cooling (i.e., reduced diabatic heating relative to SYNC) in these regions produces stationary barotropic Rossby waves that propagate far beyond the tropical SH. These stationary Rossby waves and those forced directly by the summer heating in the tropical NH are spatially phased to strengthen the southern subtropical anticyclones over all three oceans.

It is argued that the stationary barotropic Rossby waves forced directly by heating in the tropical NH have a generally weaker influence on the southern subtropical anticyclones than those forced by cooling in the equatorial oceans and the tropical SH. However, the simple two-level model used to arrive at that conclusion excludes nonlinear effects. Therefore, further analyses are needed to clarify this point. A potentially promising method is to prescribe localized heating profiles in a fully nonlinear AGCM (e.g., Jang and Strauss, 2012).

The subtropical anticyclones over the South Atlantic and South Indian Oceans could be still strengthened during the austral winter without the NH convective heating (Fig. 4h and i). It appears that in the absence of the NH heating the equatorial oceans, especially the equatorial Indian Ocean, could drive rising motions aloft to force subsidence motions over the broad regions of South Atlantic and southwestern Indian Ocean (see Fig. 6b), and thus increase SLPs therein.

The results of this study leave open some important scientific questions, which deserve future investigations. For instance, in our AGCM experiments the model SSTs in the SH are not allowed to respond to (or to the lack of) the interhemipsheric teleconnections. Therefore, it remains to be determined if and how our conclusions are modified if thermal and dynamic interactions with the surface ocean mixed layer are activated. An important and related point is that the trade winds over the SH are closely linked to the southern subtropical anticyclones. An enhanced southern subtropical anticyclone during the boreal summer could potentially increase the trade winds in the SH, and thus affect surface ocean dynamics and SSTs in the tropical SH. To explore potential air-sea interactions involving the interhemispheric teleconnections, the next step is to perform experiments of the CTRL and SYNC type with CAM4 coupled to a slab ocean mixed layer model over the SH.

Acknowledgments. We would like to thank three anonymous reviewers for their thoughtful comments and suggestions, which led to a significant improvement of the paper. We also would like to thank Teresa Losada, Xiao Heng, and Xuan Ji for their helpful comments and contributions through our science discussions between the University of Miami and UCLA, and Marlos Goes and George Halliwell for their useful comments and suggestions. This work was supported by grants from the National Science Foundation (NSF) and the National Oceanic and Atmospheric Administration (NOAA)'s Climate Program Office, and by the base funding of NOAA Atlantic Oceanographic and Meteorological Laboratory (AOML).

REFERENCES

Branstator, G., 1983: Horizontal energy propagation in a barotropic atmosphere with meridional and zonal structure. *J. Atmos. Sci.*, **40**, 1689–1708.

Chen, P., M. P. Hoerling, and R. M. Dole, 2001: The origin of the subtropical anticyclones. *J. Atmos. Sci.*, **58**, 1827–1835.

Chen, T.-C., 2003: Maintenance of summer monsoon circulations: A planetary-scale perspective. *J. Climate*, **16**, 2022–2037.

Dima, I. M., and J. M. Wallace, 2003: On the seasonality of the Hadley cell. *J. Atmos. Sci.*, **60**, 1522-1527.

Dima, I. M., J. M. Wallace, I. Kraucunas, 2005: Tropical zonal momentum balance in the NCEP reanalyses. *J. Atmos. Sci*., **62**, 2499-2513.

Gill, A. E., 1980: Some simple solutions for heat-induced tropical circulation. *Quart. J. Roy. Meteor. Soc*., **106**, 447–462.

Horel, J. D., and J. M. Wallace, 1981: Planetary-scale atmospheric phenomena associated with the Southern Oscillation. *Mon. Wea. Rev*., **109**, 813–829.

Hoskins, B. J., and D. J. Karoly, 1981: The steady linear response of a spherical atmosphere to thermal and orographic forcing. *J. Atmos. Sci*., **38**, 1179–1196.

Jang, Y., D. M. Straus, 2012: The Indian monsoon circulation response to El Niño diabatic heating. *J. Climate*, **25**, 7487–7508.

Ji, X., J. D. Neelin, S.-K. Lee, and C. R. Mechoso, 2013: Interhemispheric teleconnections from tropical heat sources in intermediate and simple models. *J. Climate*, in-revision.

Kraucunas, I., and D. L. Hartmann, 2007: Tropical stationary waves in a nonlinear shallow-water model with realistic basic states. *J. Atmos. Sci.*, **64**, 2540-2557.

Lee, S.-K., C. Wang, and B. Mapes, 2009: A simple atmospheric model of the local and teleconnection responses to heating anomalies. *J. Climate*, **22**, 272-284.

Liu, F., and B. Wang, 2013: Mechanisms of global teleconnections associated with the Asian summer monsoon: An intermediate model analysis. *J. Climate*, **26**, 1791–1806.

Liu, Y. M., G. X. Wu, and R. Ren, 2004: Relationship between the subtropical anticyclone and diabatic heating. *J. Climate*, 17, 682–698.

Matsuno, T., 1966: Quasi-geostrophic motions in the equatorial area. *J. Meteor. Soc. Japan*, **44**, 25–43.

Miyasaka, T., and H. Nakamura, 2005: Structure and formation mechanisms of the Northern Hemisphere summertime subtropical highs. *J. Climate*, **18**, 5046–5065.

Miyasaka, T., and H. Nakamura, 2010: Structure and mechanisms of the Southern Hemisphere summertime subtropical anticyclones. *J. Climate*, **23**, 2115–2130.

Neale, R. B., J. Richter, S. Park, P. H. Lauritzen, S. J. Vavrus, P. J. Rasch, and M. Zhang, 2012: The mean climate of the community atmosphere model (CAM4) in forced SST and fully coupled experiments. *J. Climate*, submitted.

Neelin, J. D., and N. Zeng, 2000: A quasi-equilibrium tropical circulation model – formulation. *J. Atmos. Sci.*, **57**, 1741-1766.

Peixoto, J. P., and A. H. Oort, 1992: *Physics of Climate*. American Institute of Physics, 520 pp.

Richter, I., and C. R. Mechoso, 2004: Orographic influences on the annual cycle of Namibian stratocumulus clouds. *Geophys. Res. Lett.*, **31**, L24108.

Richter, I. and C. R. Mechoso, 2006: Orographic influences on subtropical stratocumulus. *J. Atmos. Sci.*, **63**, 2585-2601.

Richter, I., C. R. Mechoso, and A. W. Robertson, 2008: What determines the position and intensity of the South Atlantic anticyclone in austral winter? - An AGCM study. *J. Climate*, **21**, 214–229.

Rodwell, M. J., and B. J. Hoskins, 1996: Monsoons and the dynamics of deserts. *Q. J. Roy. Meteorol. Soc.*, **122**, 1385-1404.

Rodwell, M. J., and B. J. Hoskins, 2001: Subtropical anticyclones and summer monsoons. *J. Climate*, **14**, 3192-3211.

Sardeshmukh, P. D., and B. J. Hoskins, 1988: The generation of global rotational flow by steady idealized tropical divergence. *J. Atmos. Sci*., **45**, 1228–1251.

Seager, R., R. Murtugudde, N. Naik, A. Clement, N. Gordon, and J. Miller, 2003: Air sea interaction and the seasonal cycle of the subtropical anticyclones. *J. Climate*, **16,** 1948-1966.

Ting, M., and I. M. Held, 1990: The stationary wave response to tropical SST anomaly in an idealized GCM. *J. Atmos. Sci.*, **47**, 2546–2566.

Ting, M., 1994: Maintenance of northern summer stationary waves in a GCM. *J. Atmos. Sci.*, **51**, 3286–3308.

Wang, C., S.-K. Lee, and C. R. Mechoso, 2010: Interhemispheric influence of the Atlantic warm pool on the southeastern Pacific. *J. Climate*, **23**, 404-418.

Watterson, I. G., and E. K. Schneider, 1987: The effect of the Hadley Circulation on the meridional propagation of stationary waves. *Q. J. Roy. Meteor. Soc.*, **13**, 779–813.

Figure captions:

Figure 1. Mean sea level pressure for (a) DJF and (JJA) during 1971 – 2000 from the NCEP-NCAR Reanalysis. The unit is hPa.

Figure 2. Daily solar insolation at the top of the atmosphere in (a) CTRL, (b) SYNC, and (c) CTRL – SYNC. The unit is W m^{-2}.

Figure 3. Mean sea level pressure for (a) DJF and (b) JJA from CTRL. The unit is hPa.

Figure 4. Seasonal cycle of sea level pressure averaged zonally for (a, d, and g) the South Pacific Ocean, (b, e, and h) the South Atlantic Ocean, and (c, f, and i) South Indian Ocean from the NCEP-NCAR reanalysis (top row), CTRL (middle row), and SYNC (bottom row). The unit is hPa.

Figure 5. Mean meridional overturning circulation (mass stream function) obtained from (a) CTRL, (b) SYNC, and (c) CTRL – SYNC. Circulation is clockwise (anticlockwise) around positive (negative) stream function. The unit is 10^9 Kg s^{-1}.

Figure 6. Mean velocity potential and divergent wind vector at 200 hPa from (a) CTRL, (b) SYNC, and (c) CTRL - SYNC. The units are 10^7 m^2 s^{-1} for velocity potential, and m s^{-1} for divergent wind vector.

Figure 7. (a) Mean sea level pressure, (b) stream function and wind vector at 500 hPa from CTRL - SYNC. The zonal line at 40°S roughly marks the southern end of the southern subtropical anticyclones in JJA. The stream function sign is reversed in such a way that circulation is anticlockwise around positive stream function. The units are hPa for sea level pressure, 10^7 m^2 s^{-1} for stream function, and m s^{-1} for wind vector.

Figure 8. Mean moist convective heating rate at 500 hPa for JJA from CTRL - SYNC. The unit is K day^{-1}. The three regions of diabatic heating in the NH, namely the northwestern Pacific Ocean affected by summer expansion of the western Pacific warm pool, the, and the Indian summer monsoon region are indicated by red borderlines. The three regions of diabatic cooling in the equatorial oceans and the tropical SH, namely the south-central Pacific, the western equatorial Atlantic, and the equatorial Indian Ocean are shown with blue borderlines.

Figure 9. Zonally averaged climatological (a) barotropic zonal, (b) baroclinic zonal and (c) baroclinic meridional winds in JJA obtained from SYNC (solid lines), CTRL (long-dashed lines) and the NCEP-NCAR reanalysis (short-dashed line). The barotropic zonal winds are obtained by vertically averaging the zonal winds in the troposphere (100 ~ 1000 hPa). To compute the baroclinic zonal winds, the zonal winds are vertically averaged separately for the upper troposphere (100 ~ 500 hPa) and for the lower troposphere (500 ~ 1000 hPa), and the latter is subtracted from the former then divided by 2. The same methodology is used to compute the baroclinic meridional winds.

Figure 10. Barotropic stream function and wind vector responses in the simple model experiments to the moist convective heating and cooling derived from CTRL – SYNC. The units are 10^7 m^2 s^{-1} for stream function, and m s^{-1} for wind vector.

Figure 11. Barotropic stream function and wind vector responses in the simple model experiments to diabatic cooling in (a) the central South Pacific Ocean, (b) the western equatorial Atlantic Ocean, and (c) the equatorial Indian Ocean. The units are 10^7 m^2 s^{-1} for stream function, and m s^{-1} for wind vector.

Figure 12. Barotropic stream function and wind vector responses in the simple model experiments to diabatic heating in (a) the northwestern Pacific Ocean, (b) the WHWP, and (c) the Indian summer monsoon region. The units are 10^7 m^2 s^{-1} for stream function, and m s^{-1} for wind vector.

Figure 13. Sketch of the physical processes linking the major summer monsoons in the NH and the southern subtropical anticyclones. The three regions of rising motion, the three regions of sinking motion and the regions of southern subtropical anticyclones affected are filled with gray, sky blue and red colors, respectively. The sinking regions in the southeastern tropical Pacific and the southeastern tropical Atlantic are indicated by sky blue borderlines. Thick black arrows represent divergent winds in the upper level, while light green arrows represent the ray paths of the stationary barotropic Rossby waves forced by diabatic cooling over the three regions of sinking motion and by diabatic heating in the Indian summer monsoon region.

Manuscript (figures)
Click here to download Manuscript (non-LaTeX): lee_etal_2013_jcl_figure_2nd_revision.doc

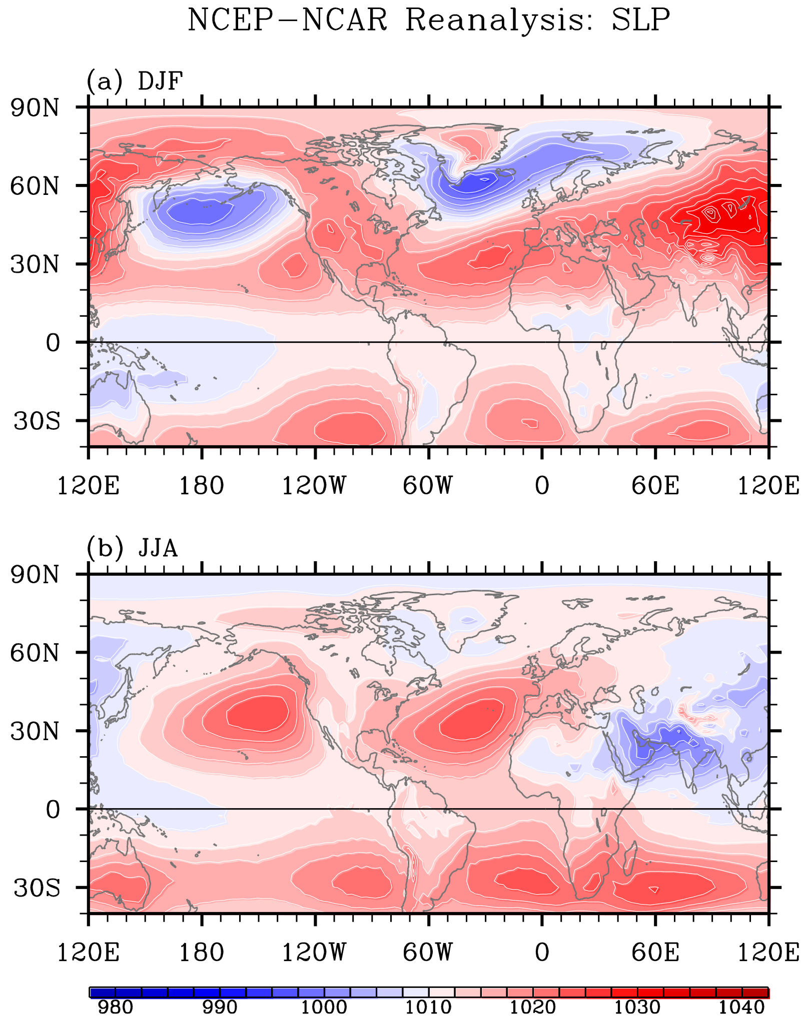

Figure 1. Mean sea level pressure for (a) DJF and (JJA) during 1971 - 2000 from the NCEP-NCAR Reanalysis. The unit is hPa.

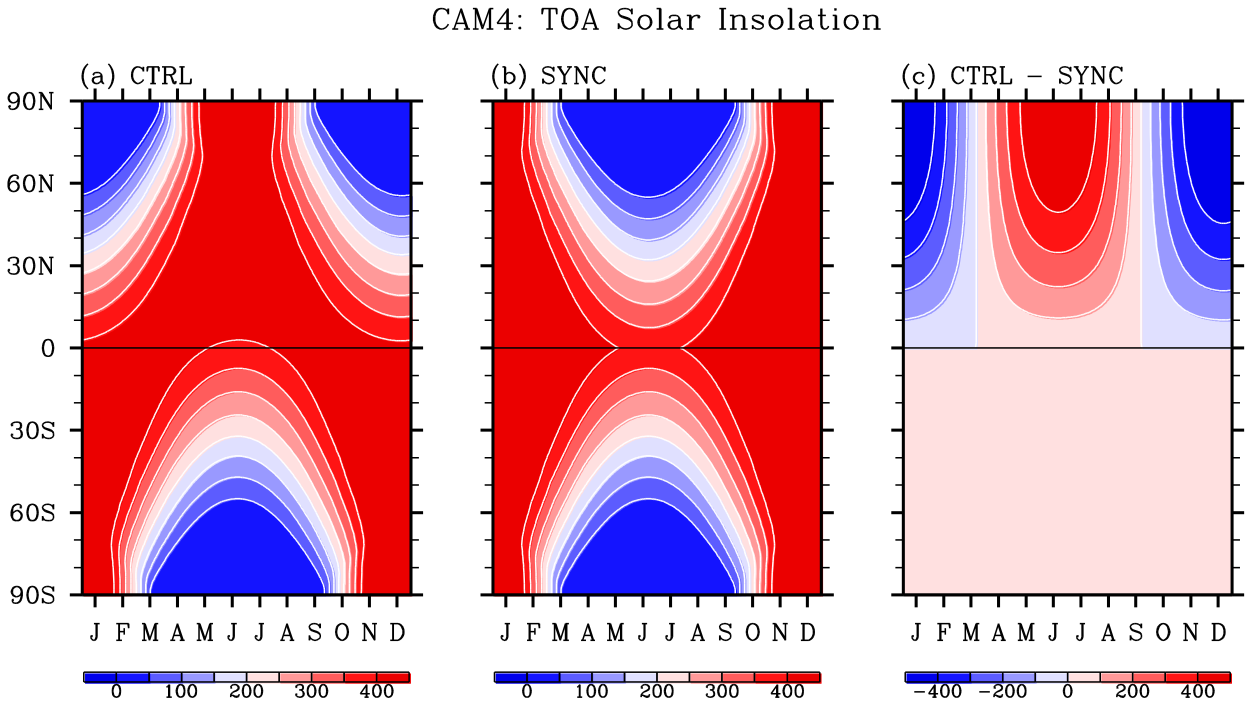

Figure 2. Daily solar insolation at the top of the atmosphere in (a) CTRL, (b) SYNC, and (c) CTRL – SYNC. The unit is W m^{-2}.

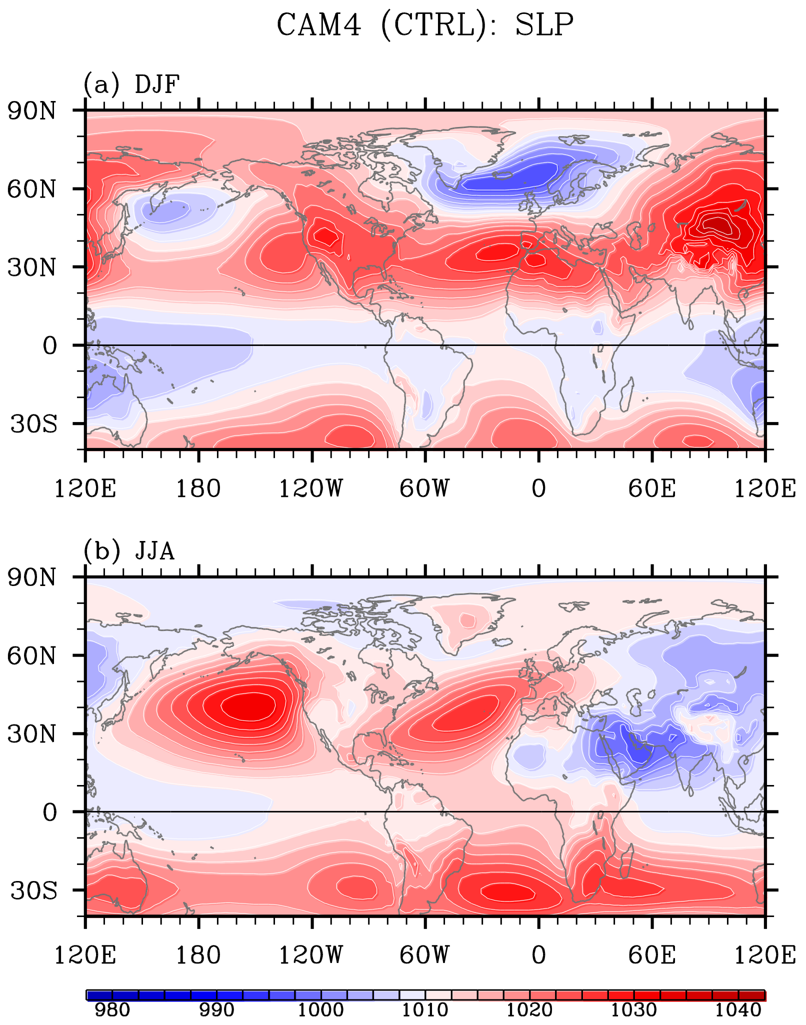

Figure 3. Mean sea level pressure for (a) DJF and (b) JJA from CTRL. The unit is hPa.

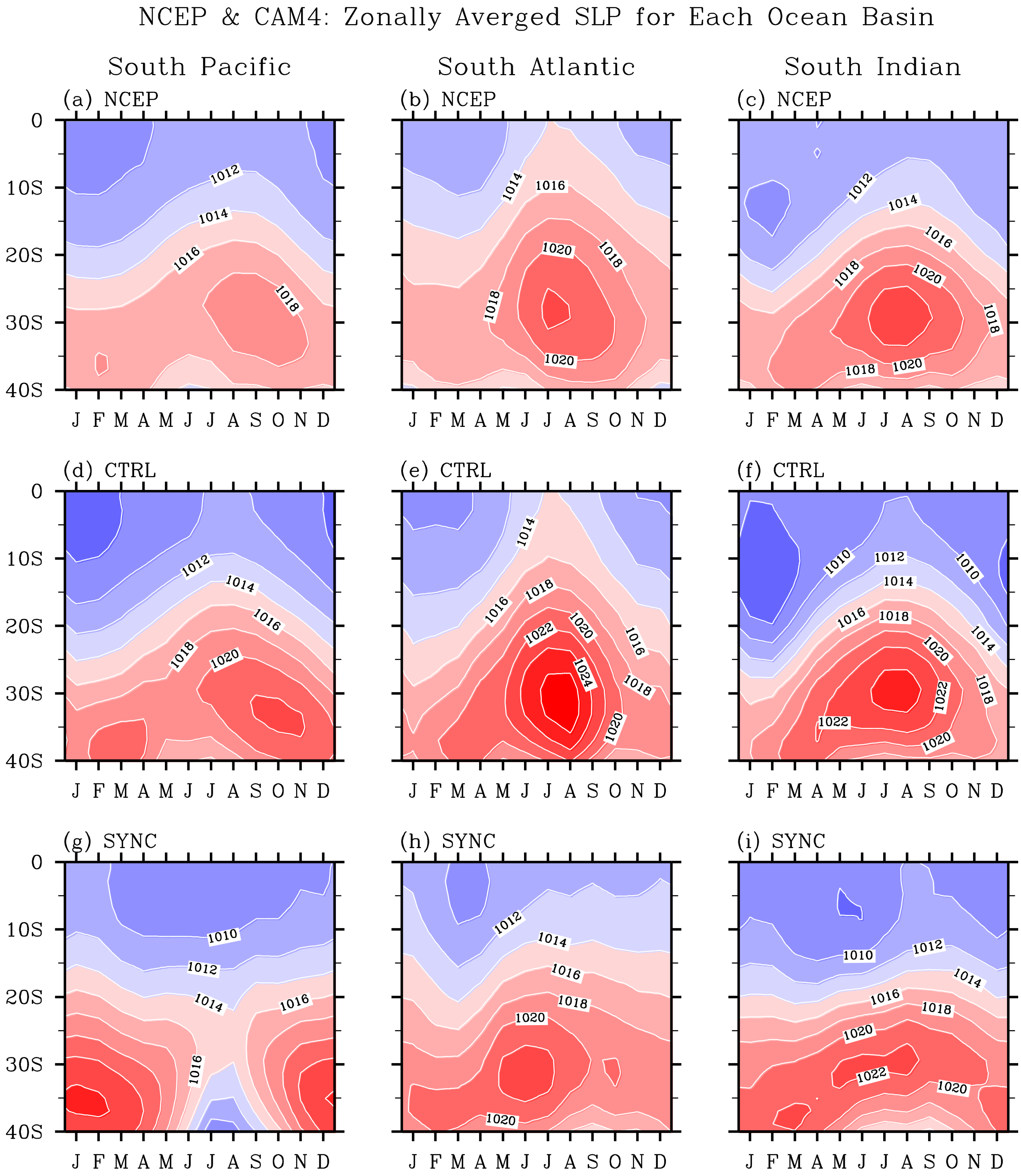

Figure 4. Seasonal cycle of sea level pressure averaged zonally for (a, d, and g) the South Pacific Ocean, (b, e, and h) the South Atlantic Ocean, and (c, f, and i) South Indian Ocean from the NCEP-NCAR reanalysis (top row), CTRL (middle row), and SYNC (bottom row). The unit is hPa.

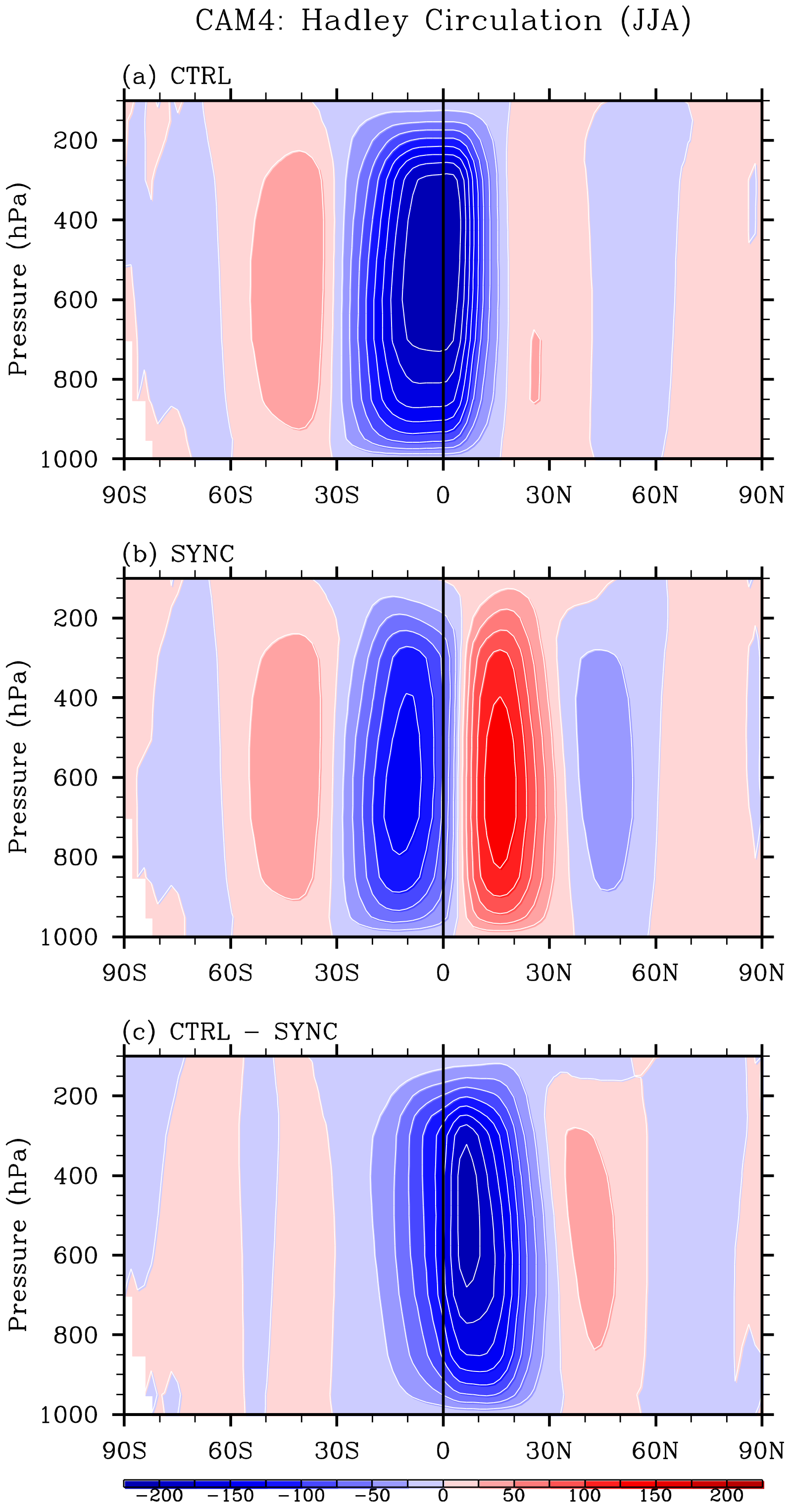

Figure 5. Mean meridional overturning circulation (mass stream function) from (a) CTRL, (b) SYNC, and (c) CTRL – SYNC. Circulation is clockwise (anticlockwise) around positive (negative) stream function. The unit is 10^9 Kg s^{-1}.

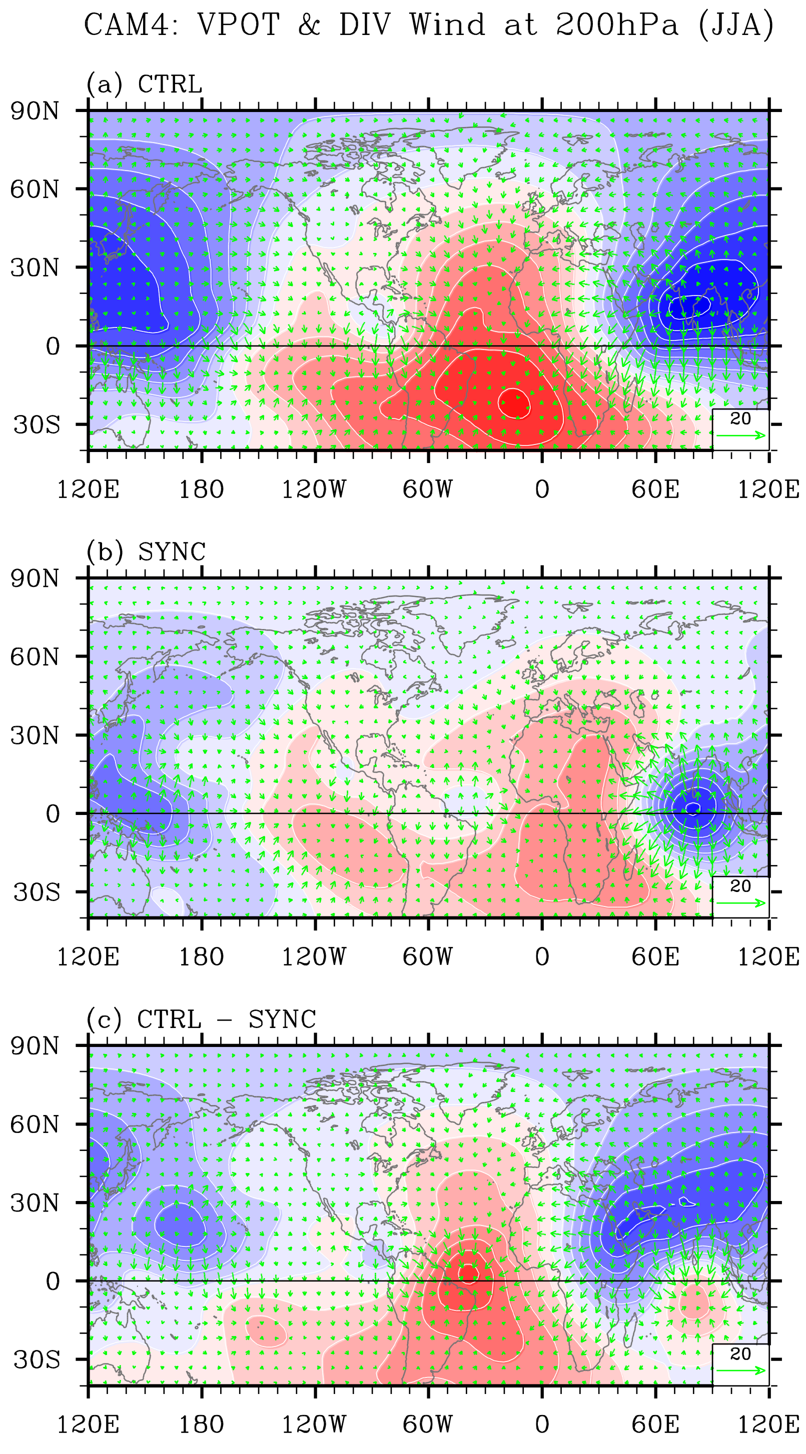

Figure 6. Mean velocity potential and divergent wind vector at 200 hPa obtained from (a) CTRL, (b) SYNC, and (c) CTRL - SYNC. The units are 10^7 m^2 s^{-1} for velocity potential, and m s^{-1} for divergent wind vector.

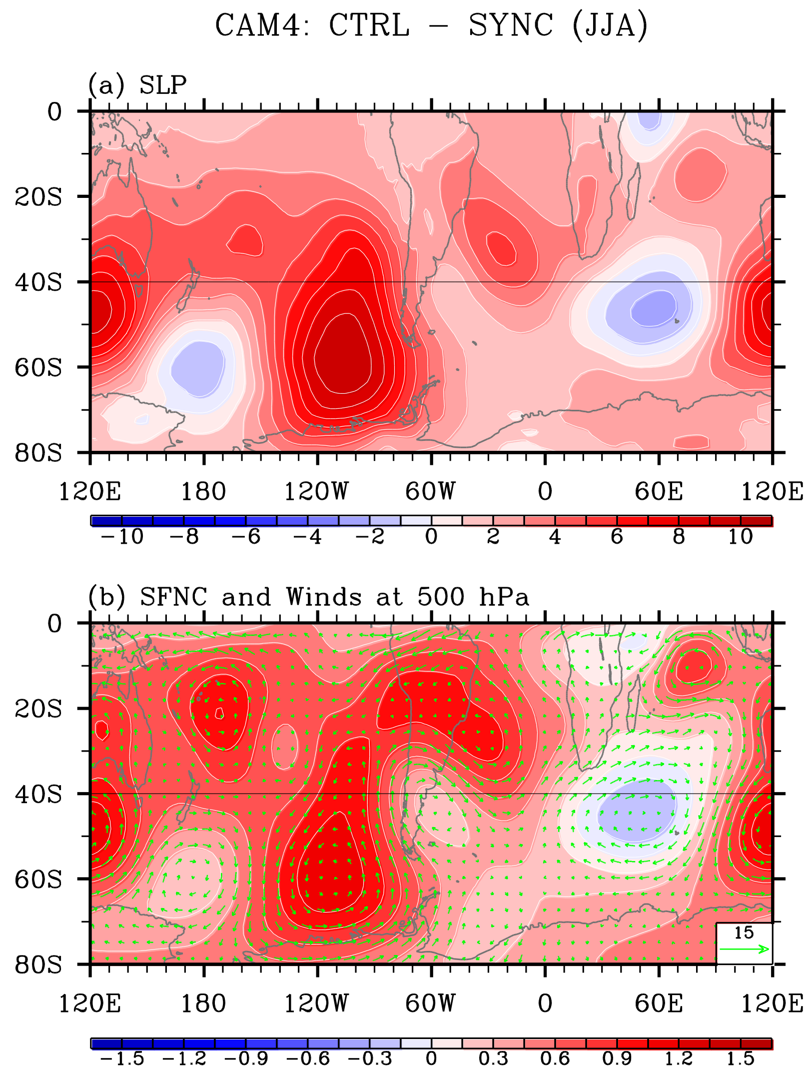

Figure 7. (a) Mean sea level pressure, (b) stream function and wind vector at 500 hPa from CTRL - SYNC. The zonal line at 40°S roughly marks the southern end of the southern subtropical anticyclones in JJA. The stream function sign is reversed in such a way that circulation is anticlockwise around positive stream function. The units are hPa for sea level pressure, m for geopotential, and m s^{-1} for wind vector.

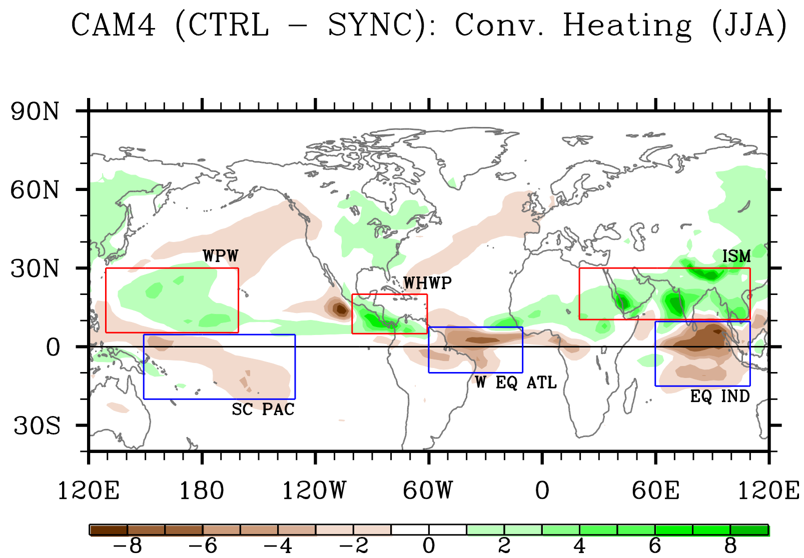

Figure 8. Mean moist convective heating rate at 500 hPa for JJA from CTRL - SYNC. The three regions of diabatic heating in the NH, namely the northwestern Pacific Ocean affected by summer expansion of the western Pacific warm pool, the WHWP, and the Indian summer monsoon region are indicated by red borderlines. The three regions of diabatic cooling in the equatorial oceans and the tropical SH, namely the south-central Pacific, the western equatorial Atlantic, and the equatorial Indian Ocean are shown with blue borderlines. The unit is K day^{-1}.

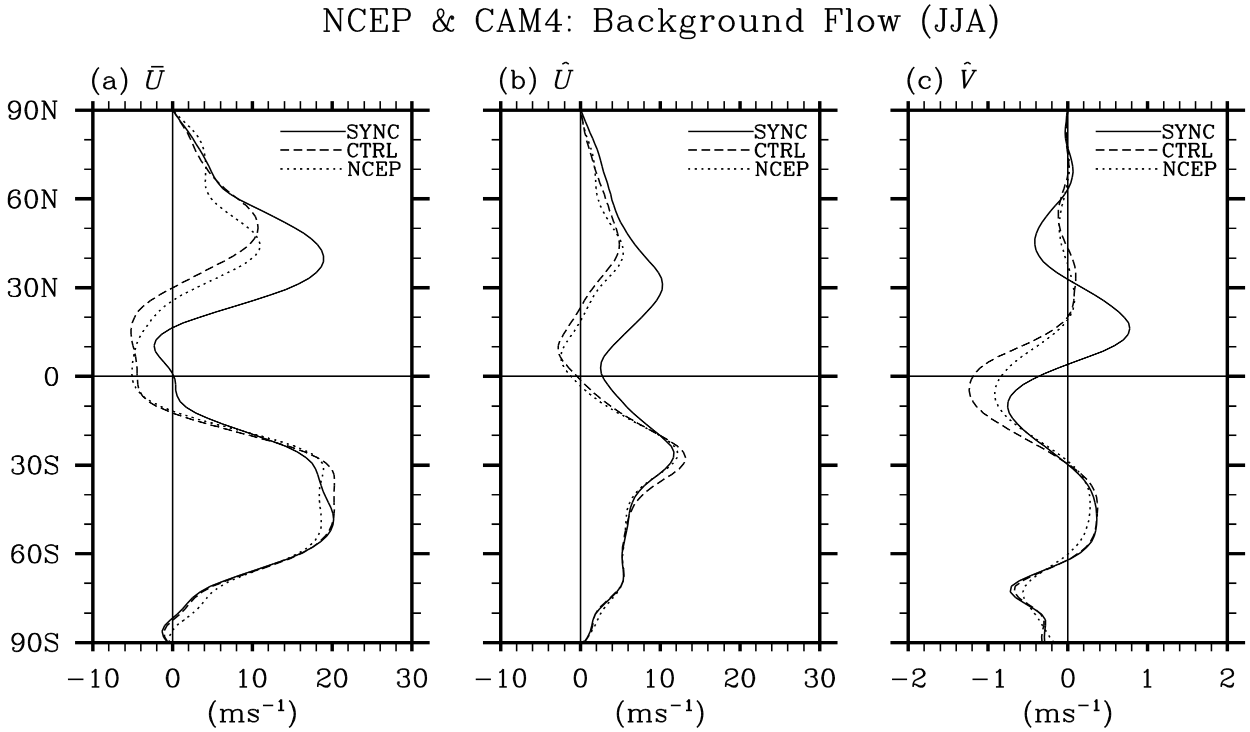

Figure 9. Zonally averaged climatological (a) barotropic zonal, (b) baroclinic zonal and (c) baroclinic meridional winds in JJA obtained from SYNC (solid lines), CTRL (long-dashed lines) and the NCEP-NCAR reanalysis (short-dashed line). The barotropic zonal winds are obtained by vertically averaging the zonal winds in the troposphere (100 ~ 1000 hPa). To compute the baroclinic zonal winds, the zonal winds are vertically averaged separately for the upper troposphere (100 ~ 500 hPa) and for the lower troposphere (500 ~ 1000 hPa), and the latter is subtracted from the former then divided by 2. The same methodology is used to compute the baroclinic meridional winds.

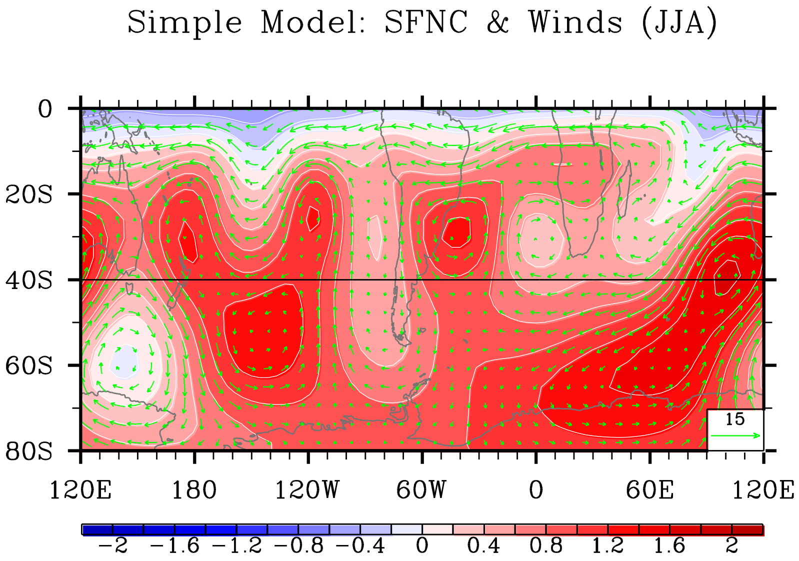

Figure 10. Barotropic stream function and wind vector responses in the simple model experiments to the moist convective heating and cooling derived from CTRL – SYNC. The units are 10^7 m^2 s^{-1} for stream function, and m s^{-1} for wind vector.

Simple Model: SFNC & Winds (JJA)

(a) South−central Pacific Ocean

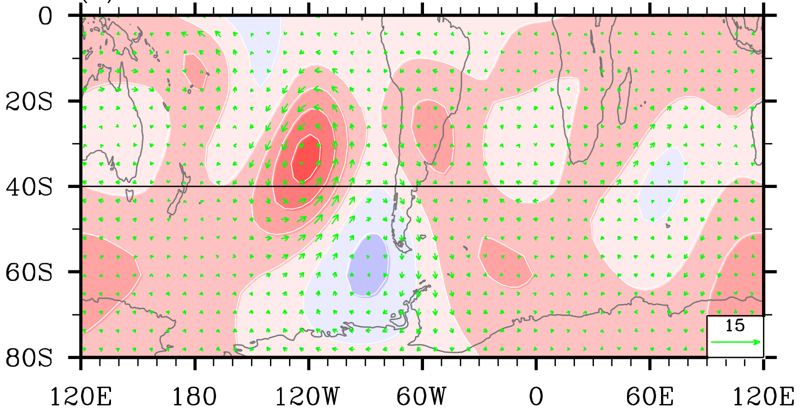

(b) Western Equatorial Atlantic Ocean

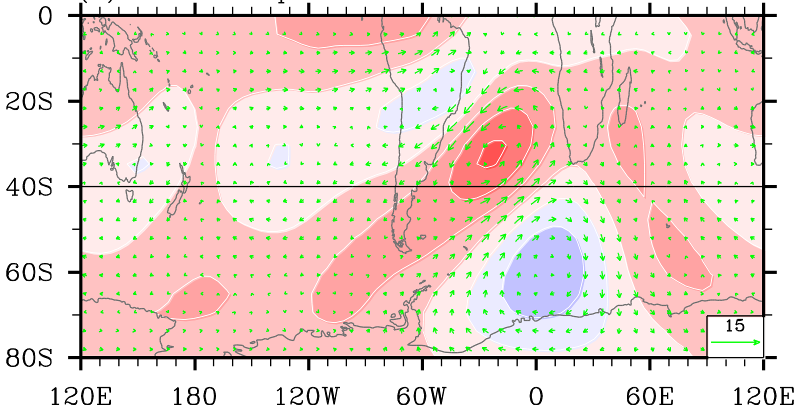

(c) Equatorial Indian Ocean

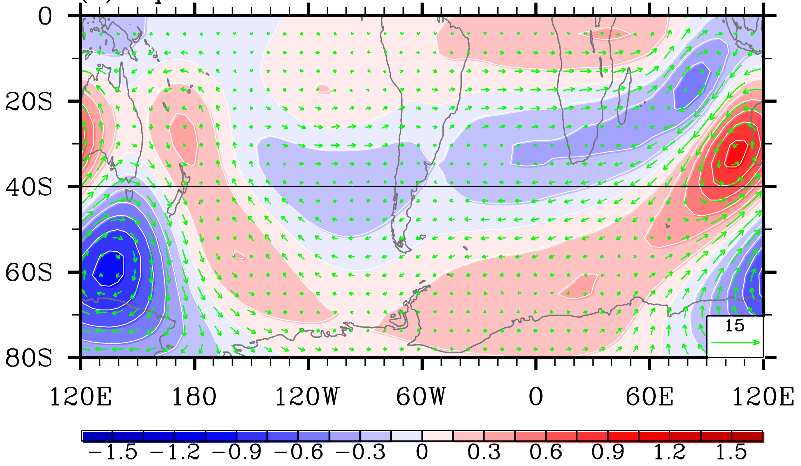

Figure 11. Barotropic stream function and wind vector responses in the simple model experiments to diabatic cooling in (a) the central South Pacific Ocean, (b) the western equatorial Atlantic Ocean, and (c) the equatorial Indian Ocean. The units are 10^7 m^2 s^{-1} for stream function, and m s^{-1} for wind vector.

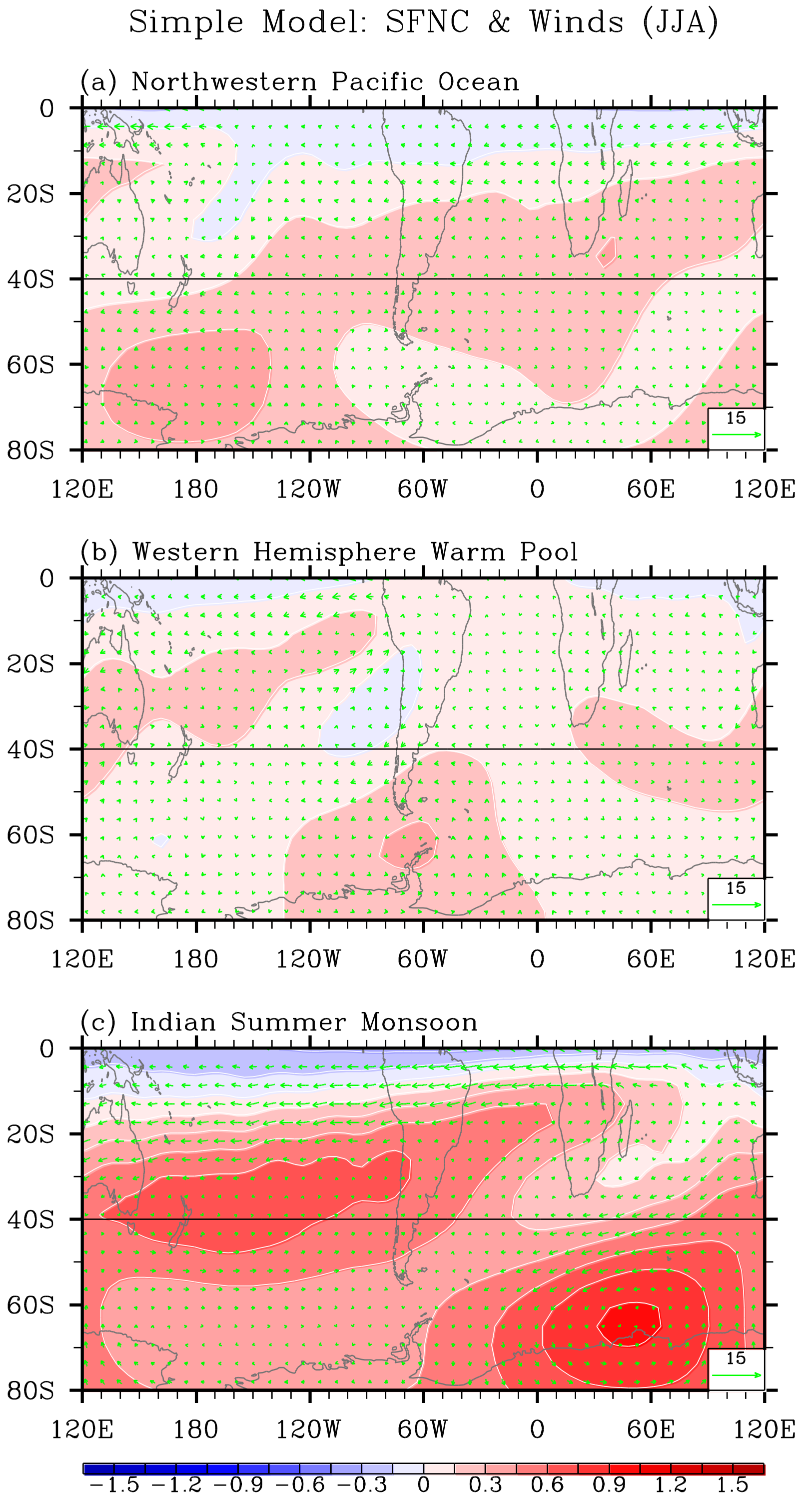

Figure 12. Barotropic stream function and wind vector responses in the simple model experiments to diabatic cooling in (a) the northwestern Pacific Ocean, (b) the WHWP, and (c) the Indian summer monsoon region. The units are 10^7 m^2 s^{-1} for stream function, and m s^{-1} for wind vector.

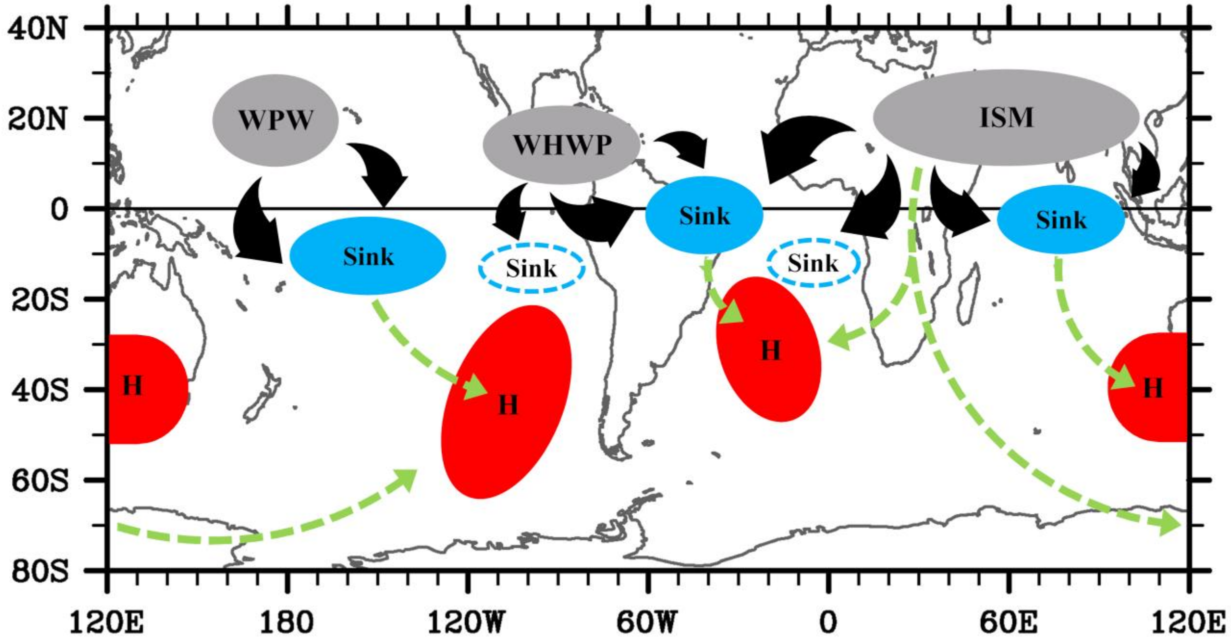

Figure 13. Sketch of the physical processes linking the major summer monsoons in the NH and the southern subtropical anticyclones. The three regions of rising motion, the three regions of sinking motion and the regions of southern subtropical anticyclones affected are filled with gray, sky blue and red colors, respectively. The sinking regions in the southeastern tropical Pacific and the southeastern tropical Atlantic are indicated by sky blue borderlines. Thick black arrows represent divergent winds in the upper level, while light green arrows represent the paths of the stationary barotropic Rossby waves forced by diabatic cooling over the three regions of sinking motion and by diabatic heating in the Indian summer monsoon region.

Figure-1 (Color)
Click here to download Non-Rendered Figure: fig01.eps

Figure-2 (Color)
Click here to download Non-Rendered Figure: fig02.eps

Figure-3 (Color)

Click here to download Non-Rendered Figure: fig03.eps

Figure-4 (Color)
Click here to download Non-Rendered Figure: fig04.eps

Figure-5 (Color)
Click here to download Non-Rendered Figure: fig05.eps

Figure-6 (Color)

Click here to download Non-Rendered Figure: fig06.eps

Figure-7 (Color)

Click here to download Non-Rendered Figure: fig07.eps

Figure-8 (Color)
Click here to download Non-Rendered Figure: fig08.eps

Figure-9 (B&W)
Click here to download Non-Rendered Figure: fig09.eps

Figure10 (Color)

Click here to download Non-Rendered Figure: fig10.eps

Figure11 (Color)
Click here to download Non-Rendered Figure: fig11.eps

Figure12 (Color)
Click here to download Non-Rendered Figure: fig12.eps

Figure13 (Color)

Click here to download Non-Rendered Figure: fig13.tif